energies

MDPI

Article

# A Decentralized Multi-Agent-Based Approach for Low Voltage Microgrid Restoration

**Ebrahim Rokrok [1], Miadreza Shafie-khah [1], Pierluigi Siano [2,*] and João P. S. Catalão [1,3,4,*]**

[1] Centre for Mechanical and Aerospace Science and Technologies (C-MAST), University of Beira Interior, R. Fonte do Lameiro, 6201-001 Covilhã, Portugal; ebrahim.rokrok@gmail.com (E.R.); miadreza@ubi.pt (M.S.-k.)

[2] Department of Industrial Engineering, University of Salerno, 84084 Fisciano (SA), Italy

[3] Institute for Systems and Computer Engineering, Technology and Science (INESC TEC), Faculty of Engineering, University of Porto, 4200-465 Porto, Portugal

[4] Institute for Systems and Computer Engineering, Research and Development (INESC-ID), Instituto Superior Técnico, University of Lisbon, Av. Rovisco Pais, 1049-001 Lisbon, Portugal

* Correspondence: psiano@unisa.it (P.S.); catalao@ubi.pt (J.P.S.C.); Tel.: +39-089-961-1111 (P.S.); +351-22-508-1850 (J.P.S.C.)

Academic Editor: Pedro Faria

Received: 11 August 2017; Accepted: 18 September 2017; Published: 27 September 2017

**Abstract:** Although a well-organized power system is less subject to blackouts, the existence of a proper restoration plan is nevertheless still essential. The goal of a restoration plan is to bring the power system back to its normal operating conditions in the shortest time after a blackout occurs and to minimize the impact of the blackout on society. This paper presents a decentralized multi-agent system (MAS)-based restoration method for a low voltage (LV) microgrid (MG). In the proposed method, the MG local controllers are assigned to the specific agents who interact with each other to achieve a common decision in the restoration procedure. The evaluation of the proposed decentralized technique using a benchmark low-voltage MG network demonstrates the effectiveness of the proposed restoration plan.

**Keywords:** average consensus algorithm (ACA); black start; local controller; microgrid (MG); multi-agent system (MAS); power system restoration (PSR)

## 1. Introduction

### 1.1. Motivations

Nowadays, the limited operating margins of the power systems have increased the risk of power blackouts and system collapse. In recent years, several major blackouts have occurred around the world. For instance, the blackout that occurred on 14 August 2003 in North America, caused an immense loss and the power system restoration (PSR) lasted nearly two weeks [1]. Also, a European power outage affected 15 million people on 4 November 2006, and it lasted up to 2 h. The blackout that occurred on 31 July 2012, in north India deenergized 50 GW of loads and affected 670 million people. The 2009 Brazil and Paraguay blackout was a power outage that occurred in many sections of Brazil and for a short time affected the entirety of Paraguay. The Fukushima nuclear power plant was faced with a series of equipment failures after the earthquake and tsunami on 11 March 2011, and a significant amount of radioactive materials were also released into ground and ocean waters [2]. When a blackout occurs, the main priority is to restore the power system in a proper manner so that the maximum load is restored as soon as possible considering the operating conditions and the system security.

During the past years, various aspects of the PSR problem have been studied, and its theories and methods are largely mature [3–7]. In conventional power systems, the restoration process begins from the transmission system by starting up those power plants which provide the black start capability in the shortest time. This allows the supply of a large part of the consumers near the power plants and to energize the transmission network [4]. The start of the restoration process from the transmission system causes many consumers in the distribution system to be supplied in the final stages of the restoration process, so the reliability of the system is decreased.

With the restructuring of the power grids toward smart grids which are based on the smart energy infrastructure consisting of microgrids (MGs) and distributed energy resources, the possibility of restoration of a large part of the loads at the distribution level along with restoration of the power plants and transmission network is provided. Therefore, the combination of the distributed energy resources and the flexible demands in the form of MGs can facilitate the implementation of local self-healing methods and accelerate the restoration process. In this sense, the PSR process can be carried out using a top-down procedure starting from the high voltage (HV) transmission system along with a bottom-up approach starting from the low voltage (LV) distribution system by using the capabilities of the LV MGs. The LV MGs and the HV transmission system will be synchronized and connect together at the medium voltage (MV) distribution level [8–11].

The motivation of this paper was to design and develop a decentralized multi-agent-based approach for restoration of a MG after a general blackout. The proposed decentralized approach provides an adequate restoration sequence to maximize the amount of restored loads.

### *1.2. Literature Review*

The aims of restoration are to enable the power system to return to its normal conditions rapidly and securely, to minimize the losses and the restoration time, and to alleviate the adverse effects on the society after an outage. Many methods and technologies are employed for preparing the restoration schemes to address the abovementioned goals. Although the nature of the outages is unique, certain common guidelines exist to help operators restore and rebuild a stable power system after an outage [12]. The PSR can be categorized based on several different criteria as follows:

(a) Different parts of the power system: PSR needs to be carried out in different types of power systems and at different levels. In [13], the restoration of the transmission system with the goal of finding an appropriate sequence of actions to minimize the size of the blackout over time is presented. To solve the restoration ordering problem (ROP), the DC model and the linear programming approximation of AC (LPAC) power flow are used, and it is shown that the DC model is not sufficiently accurate to solve the ROP. In contrast, the LPAC power flow model is sufficiently accurate to obtain the restoration plans. In [14], the PSR is stated as a multi-objective, multi-variable, and multi-constrained nonlinear optimization problem and a multi-objective model based on the combination of the multi-agent technology and Tabu search method (TSM) is proposed for the restoration of the transmission system. Some of the studies investigate the restoration of the distribution system. In [15], by using the genetic algorithm (GA), the switching operation is minimized during the restoration process. It also reduces the required calculations time. The capabilities of the distributed generations (DGs) in distribution systems are used in [16] to minimize the restoration time and maximize the amount of restored loads.

(b) Outage range: Some researchers focus on the condition in which only a small part of the power system is deenergized [13] while other researchers focus on the restoration procedure after a total blackout [17].

(c) Sub problems: Much researchers have focused on the different sub problems in PSR such as generator start-up sequence [18], standing voltage phase angles [19], and selecting suitable islands to restart [20].

(d) Modeling: There is a trade-off between speed and accuracy of PSR analysis; capturing the behavior of the real system reduces the computation time and the implementation complexity. Both static power flow calculations [17] and dynamic electromechanical models [8,21,22] are used.

Many recent reports focus on the using the capabilities of the MGs as the new effective solution for PSR at the distribution system level. In [8], the feasibility of MG restoration after a blackout is investigated using dynamic modeling. The microgrid central controller (MGCC) is responsible for making the restoration decisions such as starting-up the black start units, energizing the feeders, and restoring the loads and non-black start units. Using the information received periodically from the local controllers about generation and consumption levels, the centralized control system of the MG makes the restoration decisions. Such dynamic studies for MG restoration with the centralized approach are widely used in the literature. In [22], the restoration of the distribution system is investigated in the presence of multi-MGCC. Similar to [8], it is supposed that the sequence of the restoration actions is determined by the centralized control system. In [23] and [11], the dynamic studies of the centralized restoration process are performed for the MGs implemented in the northern region of Launceston in Tasmania, and Illinois Institute of Technology (IIT), respectively.

The centralized control schemes are low cost and easy to design, however, they suffer from single-point-failure. Furthermore, they are not adaptive to the changes of the power network structure. For instance, when new loads or generators are installed, the centralized control schemes may need to be redesigned. To avoid these shortcomings, the decentralized control scheme is introduced. One of the most popular decentralized control solutions is the multi-agent system (MAS). The MAS has the advantage of surviving single-point-failure, and it can do the decentralized data processing which, in turn, leads to task distribution and faster decision-making process [24].

MASs need to share the information process among the agents. The problem of communication of the agents can be solved by the average consensus algorithm (ACA). ACA shares the information among the agents in a distributed way to achieve an agreement on a common decision. This algorithm is widely employed in different areas including the collective behavior of swarms [25], random networks [26,27], formation flight control of multi-unmanned aerial vehicle (UAV) system [28], cooperative control of satellites [29], networks of cameras [30], and coordination and control of mobile robots [31].

### *1.3. Contributions*

This paper introduces a decentralized multi-agent-based approach for restoration of an LV MG. In the proposed scheme, the MG local controllers are assigned to specific agents. The agents only know their own local information and communicate with their neighboring agents to access the required global information. The communication among the agents for sharing the local information and accessing to the global information is based on ACA. After completing the sharing information process, all agents take a common decision based on the discovered information to determine which load or generation unit should be chosen and connected for maximizing the amount of the restored load in the shortest possible time.

The centralized restoration scheme uses the information about the last generation-consumption scenarios of the MG to determine the sequence of restoration actions. The information is periodically sent by the MG local controllers to the MGCC. After a blackout, the MGCC performs service restoration based on the latest updated information stored in a database and determines all restoration actions. Since the database information is gathered during a certain period of time before the blackout, in the case of changing in the load or generation scenario or lack of preparedness for the restoration of a generation unit or load during the restoration process, the restoration scheme will be in trouble [8,22]. Thus, there is a need for a decentralized restoration approach that uses the online information of the generation/consumption of the MG and determines a proper sequence of restoration actions to restore the maximum possible amount of loads in the shortest possible time. The proposed decentralized multi-agent based restoration approach uses the online information of the generation/consumption of the MG during the restoration process and determines a proper sequence of restoration actions.

### 1.4. Paper Organization

The rest of the paper is organized as follows: in Section 2, the centralized control structure for the black start of the MG is briefly explained. Section 3 gives the dynamic modeling of an LV MG. The employed dynamical models are compatible with the type of study. In Section 4, the proposed decentralized multi-agent based approach for the restoration of an LV MG is explained. The proposed scheme is simulated in MATLAB-Simulink (R2013b (8.2.0.701)), The MathWorks, Inc., Natick, MA, USA) environment, and the study results are presented in Section 5. Finally, Section 6 provides the conclusions.

## 2. Microgrid Control Structure for Black Start

Figure 1 shows the structure of an inverter-based LV MG. The presence of a synchronous generator in an inverter-based LV MG is not common [8]. Generally, an LV MG includes the loads, microsources (photovoltaic (PV), wind energy conversion system (WECS), fuel cell, and microturbine), and storage devices (battery energy storage systems (BESSs) and flywheels).

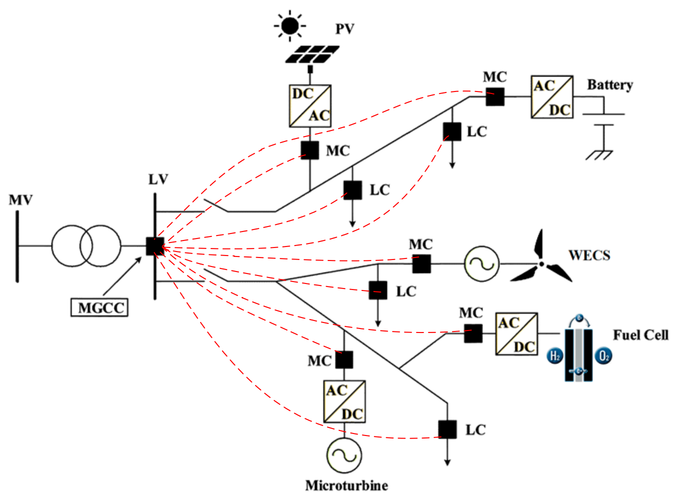


**Figure 1.** Typical low voltage (LV) microgrid (MG). MGCC: microgrid central controller; MC: microsource controller; LC: load controller; WECS: wind energy conversion system; PV: photovoltaic.

The safe, economic and stable operation of an MG in both grid connected and islanded mode depends on the existence of a proper control system [11,32–34]. An LV MG can be controlled centrally by the MGCC installed at the LV side of MV/LV substation. The load controller (LC) and microsource controller (MC) are local controllers that control the loads and microsources, respectively, and exchange the required information (such as set-points and load/consumption situations) with the MGCC through a narrow-band communication link. LC controls the loads using the local load shedding schemes in emergency conditions while MC controls the active and reactive power of microsources [35].

Under normal operation, the MG is connected to the MV network. However, in order to deal with the islanded mode and black start of the MG following a blackout, an emergency operation mode should be provided. If a blackout occurs, the restoration process time needs to be reduced as much as possible. The restoration plan is defined step by step. The main steps are building the LV network, connecting the microsources, connecting the controllable loads, controlling the voltage and frequency, and synchronizing the MG with the MV network, when it is available [8,22].

In the centralized restoration scheme, the MG black start is guided by the MGCC. The information about generation-consumption scenarios of the MG is periodically sent by the MCs and LCs to MGCC using the communication links and they will be stored in a database. After the blackout occurrence, based on the information available in the database, the MGCC determines a sequence of restoration actions and send the proper control commands to the local controllers [8,22].

To implement such a centralized restoration approach, all of the MCs and LCs must have a direct communication with the MGCC. In the case of communication failure for each local controller, the centralized restoration scheme faces with some problems. That's why it is said that the centralized control schemes easily suffer from single point failure. Moreover, the centralized restoration scheme uses the information available in its database to determine the sequence of restoration actions. Since the database information is gathered during a certain period of time before the blackout, in the case of changing in the load or generation scenario or lack of preparedness for the restoration of a generation unit or load during the restoration process, the restoration scheme will be in trouble. Thus, there is a need for a decentralized restoration approach that uses the online information of the generation/consumption of the MG and determines a proper sequence of restoration actions to restore the maximum possible amount of loads in the shortest possible time.

This paper proposes a decentralized multi-agent based approach for the MG restoration in which the online data related to the generation and consumption are used to determine a proper sequence of restoration actions. In the following sections, first, the MG components will be dynamically modeled. Then, according to the mathematical discussion on the distributed averaging problem, the proposed multi-agent based method will be presented.

## 3. Modeling of the Microgrid Components

Generally, MGs include some components such as microsources, storage devices, and loads. In order to study the dynamic behavior of the MG during the restoration process, it is essential to provide a proper dynamic model for each component that is compatible with the type of the study [36]. In the following subsections, various components of the MG are modeled.

### *3.1. Microsource Modeling*

There are several dynamic models for microsources in the literature. To model the PV cell, this paper uses the single-diode model or five-parameter model [13]. This model provides an adequate trade-off between simplicity and accuracy. A PV system is commercially available in the form of modules in which there is a number of series cells. The modules are connected in series to make a string with an appropriate voltage level. While, to increase the current rating, the strings are connected in parallel and form an array. In [37], the model of the PV array based on the five parameter model is found. In this paper, it is assumed that the PV arrays work at the maximum power point.

The WESS model used in this study is based on the constant speed wind turbine that is available in [38]. Likewise, regarding the period of study, only the average value of the wind speed is considered (i.e., the wind speed is constant).

To model the dynamic behavior of the microturbine, the gas turbine (GAST) model [39] is used. There are two types of the microturbine including single-shaft microturbine (high-speed) and split-shaft microturbine (low-speed). In the single-shaft microturbine, the turbine speed range is from 50,000 to 120,000 rpm. So, this type of microturbine requires an AC/DC/AC converter for connecting to the grid. The split-shaft microturbine uses a power turbine that is rotated at 3600 rpm and can be connected to a conventional induction generator using a gearbox [39].

Reference [40] provides a basic dynamic model for a solid-oxide fuel cell (SOFC) that is used in this paper. This model has some assumption to achieve an integrated dynamic model for using in the power systems simulations.

### *3.2. Converter Modeling*

There are two kinds of control mode for operating the converters: (1) grid-forming mode and (2) grid-following mode [41]. The grid-forming converters emulate the behavior of a synchronous generator and provide the voltage and frequency references for the MG. The grid-forming converter acts as a voltage source and controls its output voltage and frequency using the droop control. When the MG works in the islanded mode, at least one converter must operate as a grid-forming converter.

DGs must meet two requirements to have the black start capability: (i) equipped with storage devices (batteries or super-capacitors) in the DC link of their inverter and (ii) operation of their inverter in the grid-forming control mode. These DGs are capable of restarting without any external power source, energize the network, supply a part of loads, and provide remote cranking power for the other DGs with the grid-following inverter control system [42]. Figure 2 shows the control structure of a droop-based grid-forming converter.

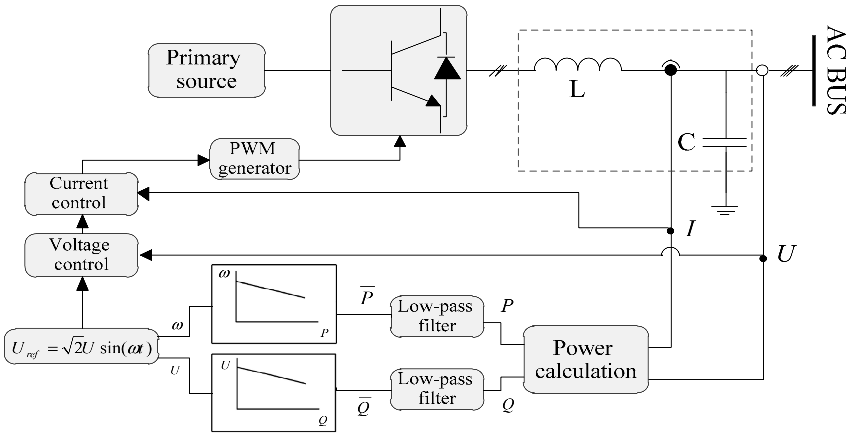


**Figure 2.** Structure of a grid-forming converter control system. PWM: Pulse width modulation.

The grid-following converters are mainly designed to deliver a pre-determined power to an energized grid. If there is no synchronous generator or grid-forming converter in the MG, the grid-following converter cannot operate. Figure 3 shows the control structure of a grid-following converter [43].

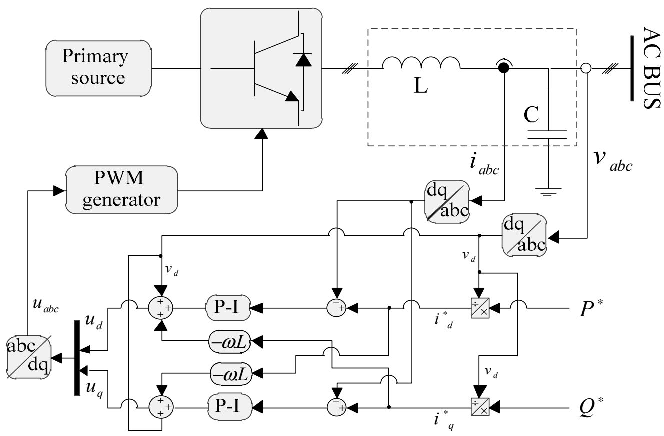


**Figure 3.** Structure of a grid-following converter control system.

## 4. Proposed Decentralized Approach

### *4.1. Mathematical Background*

The consensus problem is a prevalent problem in distributed control. In the following two subsections, the ACA is explained.

#### 4.1.1. Distributed Averaging

Let $g = (N, E)$ be a graph with $N$ nodes and $E$ edges. In node set $N = \{1, 2, \ldots, n\}$, consider each edge $\{i, j\} \in E$ is an unordered pair of distinct nodes. Let $c_i^0$ be a real number associated to node $i$ at time $t = 0$. The average consensus problem calculates iteratively the average $(1/n)\sum_{i=1}^{n} c_i^0$ in a distributed way at every node (see Figure 4). The following iterative law, known as ACA, is proposed in the literature to solve this averaging problem [44]:

$$c_i^{k+1} = c_i^k + \sum_{j \in N_i} w_{ij}(c_j^k - c_i^k), \tag{1}$$

where $i = 1, 2, \ldots, n$; $n$ is the number of nodes; $c_i^k$, $c_i^{k+1}$ are the values of node $i$ at iteration $k$ and $k + 1$, respectively, and $w_{ij}$ is the weight coefficient that enables communication between neighboring nodes $i$ and $j$. If nodes $i$ and $j$ are connected together, $0 < w_{ij} < 1$, otherwise, $w_{ij} = 0$. $N_i$ is the index of nodes connected to node $i$.

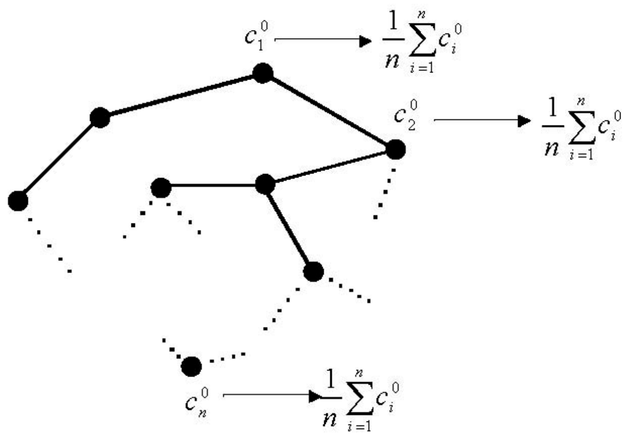

**Figure 4.** Principle of distributed averaging.

By considering $\mathbf{C^k} = [c_1^k, \ldots, c_i^k, \ldots, c_n^k]^{\mathrm{T}}$, Equation (1) can be expressed in matrix form as follows:

$$\mathbf{C_i^{k+1}} = \mathbf{C_i^k} + \mathbf{A}\mathbf{C_i^k} = (\mathbf{I} + \mathbf{A})\mathbf{C_i^k} \rightarrow \mathbf{C_i^{k+1}} = \mathbf{D}\mathbf{C_i^k}, \tag{2}$$

where $\mathbf{I}$ is the identity matrix, and:

$$\mathbf{D} = \begin{bmatrix} 1 - \sum\limits_{j \in N_1} w_{1j} & \cdots & w_{1i} & \cdots & w_{1n} \\ \cdots & \cdots & \cdots & \cdots & \cdots \\ w_{i1} & \cdots & 1 - \sum\limits_{j \in N_i} w_{ij} & \cdots & w_{in} \\ \cdots & \cdots & \cdots & \cdots & \cdots \\ w_{n1} & \cdots & w_{ni} & \cdots & 1 - \sum\limits_{j \in N_n} w_{nj} \end{bmatrix}_{n \times n}. \tag{3}$$

The square matrix $\mathbf{D}$ is said to be *doubly stochastic* if its elements are non-negative and sums of each row and each column are equal to ones, i.e., with $\mathbf{1_{1 \times n}} = [1, 1, \ldots, 1]$, $\mathbf{1} \times \mathbf{D} = \mathbf{1}$ and $\mathbf{1} \times \mathbf{D^T} = \mathbf{1}$ [45]. Based on the Gerschgorin's Disks theorem, the eigenvalues of $\mathbf{D}$ are lower than or equal to one. According to the *Perron Frobenius Lemma* [46], one can write:

$$\lim_{k \to \infty} \mathbf{D}^k = \frac{\mathbf{1}^T * \mathbf{1}}{n}, \tag{4}$$

where $n$ is the dimension of matrix $\mathbf{D}$. Combination of (2) and (4) leads to:

$$\lim_{k\to\infty} \mathbf{C}_i^k = \frac{\mathbf{1}^T * \mathbf{1}}{n}\mathbf{C}_i^0. \tag{5}$$

From Equation (5), one can see that the system reaches to consensus when $k$ approaches infinity. The speed of convergence depends on the design of $\mathbf{D}$. In practice, the exact equilibrium is not required, and the number of required steps for converging is approximately equal to:

$$k = \frac{-1}{\log_e(\frac{1}{\lambda_2})}, \tag{6}$$

where $e$ is the error tolerance and $\lambda_2$ is the second biggest eigenvalue of $\mathbf{D}$ [44]. Equation (6) shows that $\lambda_2$ determines the number of required steps to converge or equivalently the speed of the algorithm. To achieve the maximum speed and the optimal solution, the weight coefficients in matrix $\mathbf{D}$ must be determined in such a way to minimize $\lambda_2$.

#### 4.1.2. Coefficient Setting

The employed method for setting the weight coefficients depends on the type of application, i.e., offline or online applications. If the system is exposed to changes of configuration, the optimization problem must be solved again at every change. Because of the multiple variables and constraints in this optimization problem and the required time to achieve the information of the new system configuration, the optimization is time consuming and is, therefore, suitable for offline applications. For online application, there is a requirement for a proper algorithm to adjust the weight coefficients near their optimum values. Normally, in online applications, the weight coefficients are determined by using a simple rule named *Uniform* method [44]. This method proposes the fixed coefficients that are calculated as follows:

$$w_{ij} = \begin{cases} 1/n, & j \in N_i \\ 1 - \sum\limits_{j\in N_i} 1/n, & i = j \\ 0, & \text{otherwise.} \end{cases} \tag{7}$$

In above equations, $n$ is the number of nodes. To achieve a higher convergence speed, another method named *Metropolis* is introduced in [47] that makes $\lambda_2$ near to its minimum value using an adaptive weight updating law. The updating rule is:

$$w_{ij} = \begin{cases} 1/(Max(n_i, n_j) + 1), & j \in N_i \\ 1 - \sum\limits_{j\in N_i} 1/(Max(n_i, n_j) + 1), & i = j \\ 0, & \text{otherwise,} \end{cases} \tag{8}$$

where $n_i$ and $n_j$ are the number of nodes in the neighborhood of the node $i$ and $j$, respectively. It is easy to show that these two methods guarantee the two required conditions for applying the *Perron Frobenius Lemma* to $\mathbf{D}$ (i.e., the sums of each column and row of the $\mathbf{D}$ are ones, and all its eigenvalues are equal or lower than one). To make a comparison between the speeds of the ACA with various coefficient setting rules, let consider the graph depicted in Figure 5. Now, let us define the initial values assigned to each node as follows: $c_1^0 = 100$, $c_2^0 = 100$, $c_3^0 = -50$, $c_4^0 = -100$, $c_5^0 = -50$.

By using Equation (2), the equilibrium point for unlimited iterations will be:

$$c_1^\infty = c_2^\infty = c_3^\infty = c_4^\infty = c_5^\infty = \frac{1}{5}\sum_{i=1}^{5} c_i^0 = 0. \tag{9}$$

It means that after using the consensus algorithm (Equation (1)), the number '0' exists in each node. Figure 6 shows the value in each node for 60 iterations. Considering an error tolerance equal to

0.01, the nodes have reached the consensus with 31 and 25 iterations for the uniform and metropolis methods, respectively.

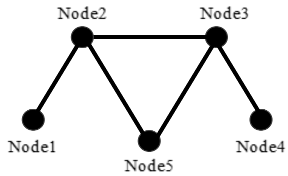


**Figure 5.** A typical studied graph.

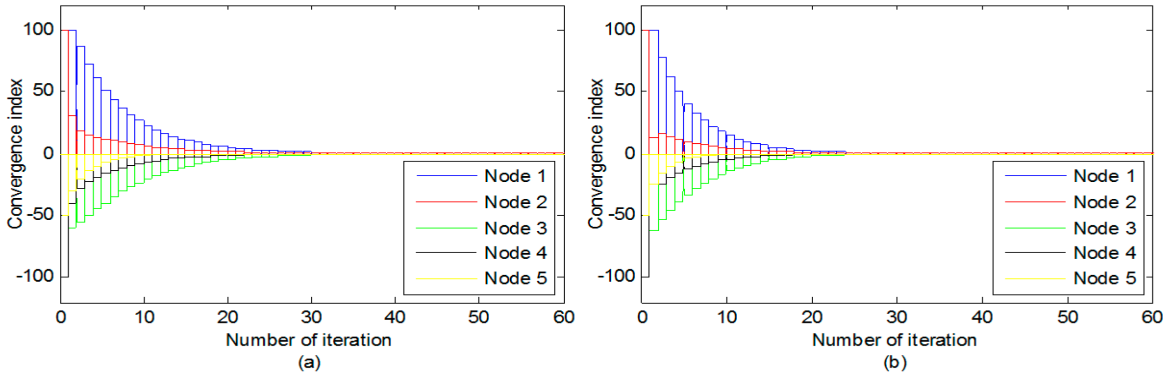


**Figure 6.** Comparison of converging speed of different methods: (**a**) uniform; (**b**) metropolis.

### *4.2. General Assumptions*

The goal of this paper is to develop a decentralized multi-agent-based approach to restore the MG loads and generations with a proper sequence of actions after a total blackout. The local controllers (MCs and LCs) and the MG communication infrastructure are so important for the successful implementation of the decentralized restoration scheme.

Based on the abovementioned distributed averaging algorithm, it is assumed that each node of the graph can be considered as an agent. The edges of the graph can be considered as the communication links among the agents. It is assumed that each local controller is assigned to a specific agent. Thus, there are two kinds of agents: (i) MC agents and (ii) LC agents. Figure 7 shows the conceptual decentralized multi-agent based model for MG restoration. In this model, each MC agent has some local information such as the amount of the generation capacity of the corresponding microsource, connection situation of the corresponding microsource (connected or disconnected), its availability and preparedness for the restoration, and pre-defined priority for the restoration.

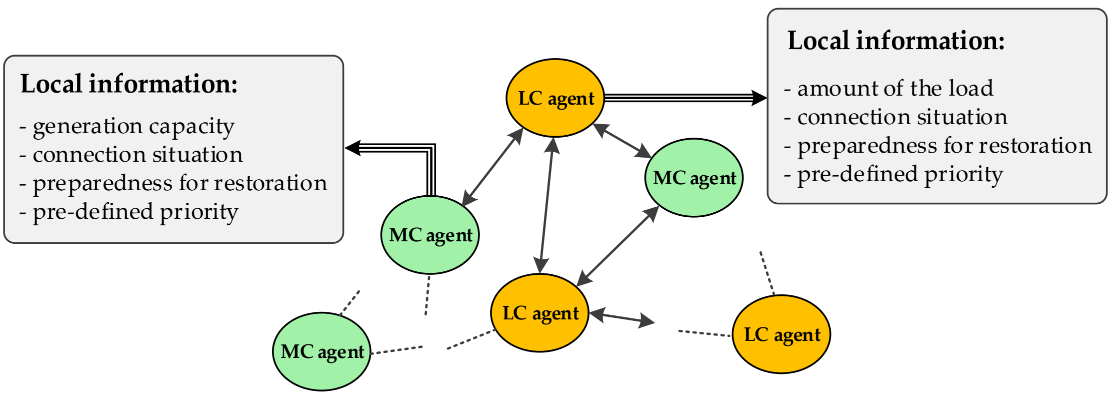


**Figure 7.** Conceptual decentralized multi-agent based model for MG restoration.

The LC agents have similar local information of their corresponding loads. The agents don't have any direct access to the global information of the system. An agent is only able to communicate with its neighbors. By using the ACA based communication law, the agents are able to share the local information, to access the global information, and accordingly to take a common decision for restoring the loads or generation units.

### 4.3. Information Sharing Process

The local initial information of each agent is placed within an initial matrix. The initial matrices just have the local information of the agents. Agent $i$ is initialized with a $n \times 4$ matrix $\mathbf{M_i}$ where $n$ is the number of agents. In $\mathbf{M_i}$, up to four non-zero elements may exist. These three non-zero elements are $M_i(i,1)$, $M_i(i,2)$, $M_i(i,3)$, and $M_i(i,4)$. $M_i(i,1)$ can be either 0 or $i$ to show whether the generation unit or the load assigned to agent $i$ is connected or not. Each agent can realize which generation units or loads are disconnected by checking the position of the zeros. $M_i(i,2)$ can be 0 or $i$ to show that the disconnected load or generation unit is ready for restoration or not. In the case of MC agents, $M_i(i,3)$ shows the amount of the power that the generation unit can produce while in the case of LC agents, it represents the amount of the load power that agent $i$ will consume. $M_i(i,4)$ can be 0, 1, 2, 3 that shows a pre-defined priority of the agents for restoration action. If $M_i(i,4) = 0$, the agent $i$ has no pre-defined priority.

For example, let consider the initial matrices $\mathbf{M_i}$, $\mathbf{M_j}$, $\mathbf{M_n}$ for agent $i$, $j$, $n$, respectively, as follows:

$$\mathbf{M_i} = \begin{bmatrix} 0 & 0 & 0 & 0 \\ \vdots & \vdots & \vdots & \vdots \\ 0 & i & P_{G_i} & 0 \\ \vdots & \vdots & \vdots & \vdots \\ 0 & 0 & 0 & 0 \end{bmatrix}_{n\times 4}, \mathbf{M_j} = \begin{bmatrix} 0 & 0 & 0 & 0 \\ \vdots & \vdots & \vdots & \vdots \\ 0 & j & -P_{L_j} & 1 \\ \vdots & \vdots & \vdots & \vdots \\ 0 & 0 & 0 & 0 \end{bmatrix}_{n\times 4}, \mathbf{M_n} = \begin{bmatrix} 0 & 0 & 0 & 0 \\ \vdots & \vdots & \vdots & \vdots \\ \vdots & \vdots & \vdots & \vdots \\ \vdots & \vdots & \vdots & \vdots \\ n & 0 & 0 & 0 \end{bmatrix}_{n\times 4}. \quad (10)$$

The above initial matrices present the following information. MC-agent $i$ is disconnected; it is ready for restoration; if it is connected, it can produce power equal to $P_{G_i}$; and it has no pre-defined priority. Similarly, the LC-agent $j$ is disconnected; it is ready for restoration; if it is connected, it consumes $P_{L_j}$; and it has the highest priority to be connected. The agent $n$ is connected, and there is no need for the restoration. Each agent has a similar principle to make the initial information matrix. By using the ACA (Equation (1)), all initial matrices will converge to the same matrix that is available for each agent. A typical final converged matrix can be:

$$\mathbf{M_{conv.}} = \begin{bmatrix} \vdots & \vdots & \vdots & \vdots \\ \frac{0}{n} & \frac{i}{n} & \frac{P_{G_i}}{n} & \frac{0}{n} \\ \vdots & \vdots & \vdots & \vdots \\ \frac{0}{n} & \frac{j}{n} & \frac{-P_{L_j}}{n} & \frac{1}{n} \\ \vdots & \vdots & \vdots & \vdots \\ \frac{n}{n} & \frac{0}{n} & \frac{0}{n} & \frac{0}{n} \end{bmatrix}_{n\times 4}. \quad (11)$$

Each element of the final converged matrix is equal to the average summation of the corresponding elements existed in the initial matrices. The actual amount of each element can be obtained by multiplying the element by $n$. According to the discovered global information ($\mathbf{M_{conv.}}$), the amount of disconnected loads and generations are available and after reaching the consensus, all agents take a common decision for restoring the loads or generation units. The following subsection is devoted to implementing the proposed method in which the function of agents and decision making process are described.

*4.4. Implementation of the Proposed Multi-Agent Based Approach for MG Restoration*

The function modules of the agent *i* is illustrated in Figure 8. Each agent has four main modules: (1) initialization; (2) information update; (3) information keep; and (4) exchange and decision making. The required steps for operation of the agents can be designated as follows:

Step 1: Initialization: in this step, the local initial information matrix of each agent ($\mathbf{M_i^0}$) is formed.
Step 2: Information sharing: in this step, each agent receives the information of its neighboring agents through a communication link and updates its information by using the ACA. After reaching the consensus, the common decision will be made.
Step 3: Decision making: when the agents reach the consensus in the sharing information process, a proper decision will be made. Decision making is one of the crucial parts of the agents' function blocks. This block must be designed to meet the initial restoration steps such as setting up the generation units with black start capability and energizing the restoration path. Moreover, in the next steps, this block must determine a proper sequence for connection of disconnected loads and generation units by providing the maximum amount of the restored loads in the shortest possible time.

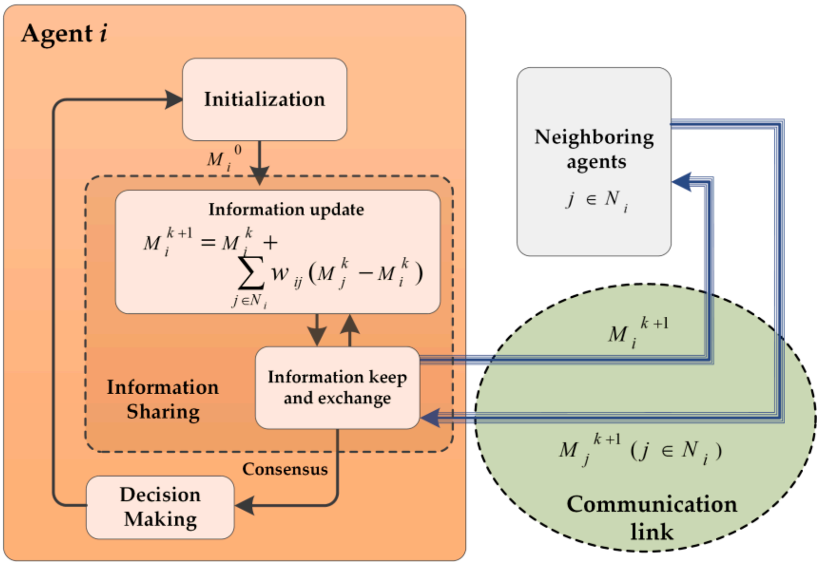


**Figure 8.** Function of agent *i* for MG restoration.

Decision Making Process

MG restoration process begins by setting up a generation unit with black start capability. In an inverter-based MG, the inverter with grid-forming control mode has the black start capability. It is assumed that in the MG, one inverter is in grid-forming control mode and the other ones operate in grid following mode. The output real power of the grid-following inverters is a constant value. However, the output real power of the grid-forming inverter varies based on the MG frequency (droop control). During the restoration process, the connection of a load or a generation unit changes the output power of the grid-forming inverter. The capacity and the instantaneous power of grid-forming inverter play a key role in determining a proper sequence of connecting the loads and generation units with a grid-following inverter.

To help better understand this, consider the flowchart of the decision making process shown in Figure 9. When the algorithm is run for the first time, the microsource with grid forming inverter is chosen and connected to energize the MG feeder. Then, a pre-defined interruption is required for damping of the frequency fluctuations. The interruption time depends on the inertia and damping factor of the MG. In the next run of the algorithm, after reaching the consensus, the information related to the output power of the grid-forming inverter $P_{\text{form}}$ that is a small value (only for energizing the MG feeder) as well as the disconnected load units and available power of the generation units with grid-following inverter are available for all agents. The capacity of the grid-forming inverter $P_{\text{form}}^{\text{cap}}$ is also specified. In this step, based on the discovered information, the largest possible amount of the load is chosen to be connected. This amount of the connected load makes the grid-forming inverter to work in the capacity limits, so in the next step, a generation unit with the grid-following inverter is chosen to releases the capacity of the grid-forming inverter by providing a fixed amount of power. This procedure will continue until all of the generation units and the maximum possible amount of the loads are connected.

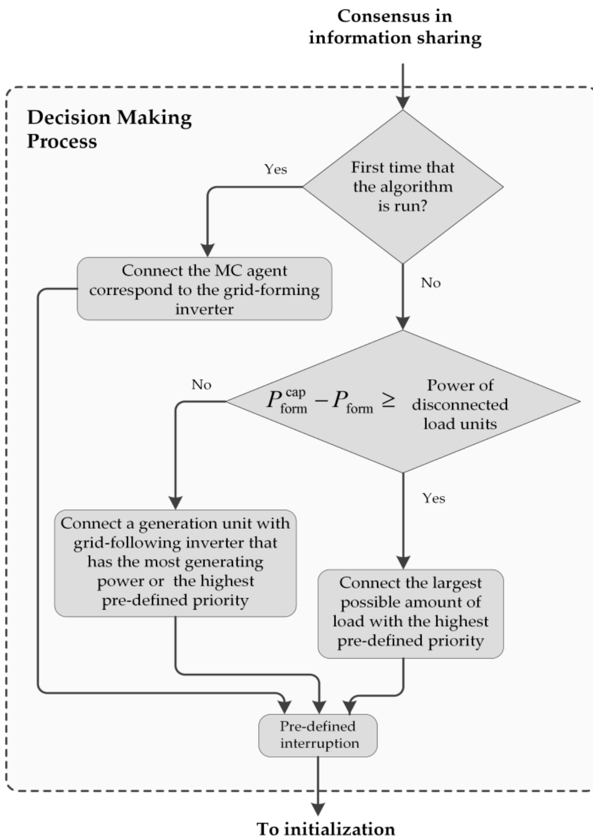


**Figure 9.** Flowchart of the decision making process.

## 5. Simulation Results and Discussion

In order to evaluate the dynamic behavior of an MG during restoration procedure, a benchmark LV MG network presented in Figure 10 is implemented in the simulation platform. The electrical data for this LV test system can be found in [48]. It is supposed that the MG is subjected to a total blackout. The studied MG includes nine local controllers, and each one is assigned to a specific agent. Figure 11 shows the two topologies for connection of the agents.

From (6), it can be observed that the speed of ACA is independent of the initial information matrix and it depends on how the agents are connected and how the weight coefficients are determined.

To verify the convergence speed of the ACA for the topologies of Figure 11, let define the initial values assigned to each agent as follows:

$$c_1^0 = 1, c_2^0 = -1, c_3^0 = 1, c_4^0 = -1, c_5^0 = 1, c_6^0 = -1, c_7^0 = 1, c_8^0 = -1, c_9^0 = 0. \quad (12)$$

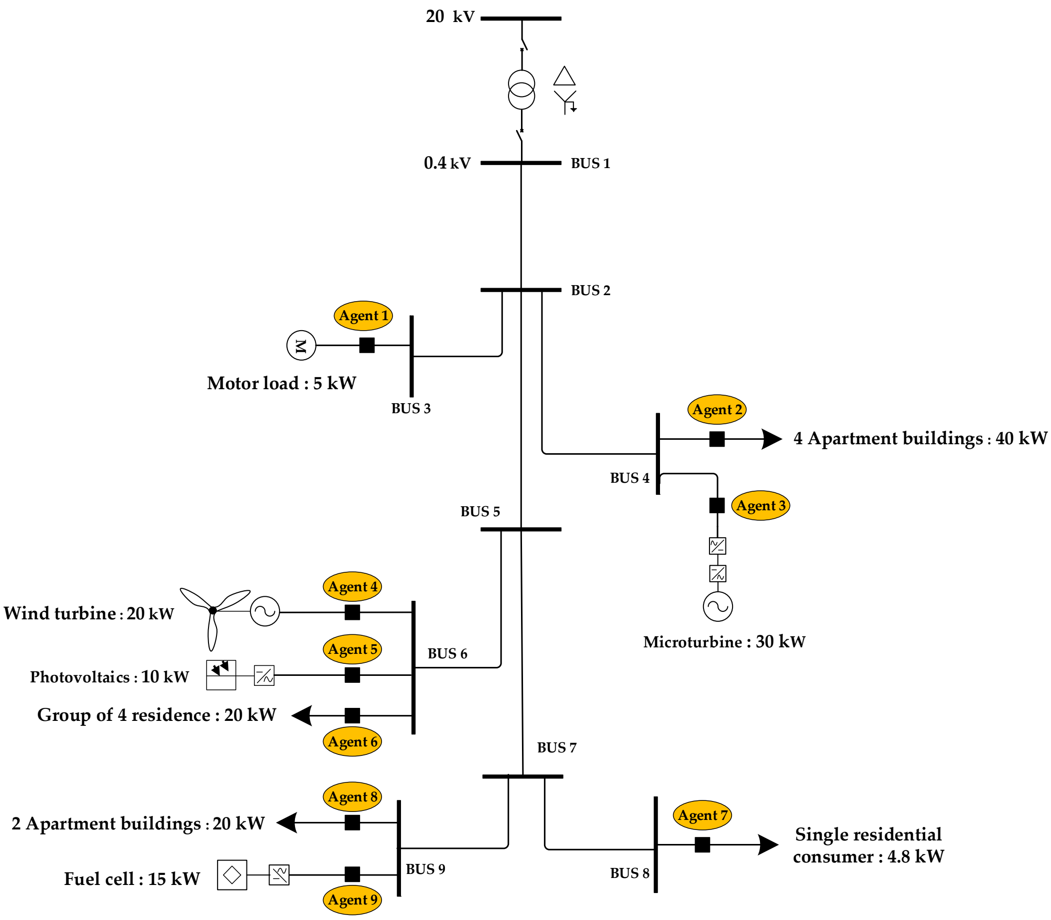


**Figure 10.** Benchmark LV MG network.

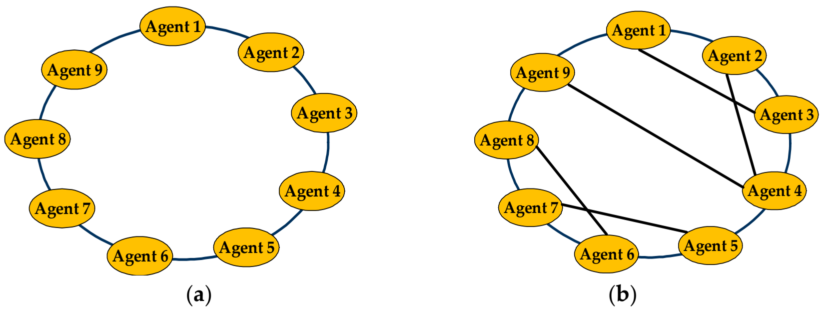


**Figure 11.** Different topologies for connection of the local controller agents: (**a**) topology a; (**b**) topology b.

By using Equation (2), the equilibrium point for unlimited iterations will be:

$$c_1^\infty = c_2^\infty = c_3^\infty = c_4^\infty = c_5^\infty = c_6^\infty = c_7^\infty = c_8^\infty = c_9^\infty = \frac{1}{9}\sum_{i=1}^{9} c_i^0 = 0. \quad (13)$$

It means that after using the consensus algorithm (Equation (1)), the number '0' exists in each agent. The metropolis method is used for determining the weight coefficient. Figure 12 shows the value in each agent for 40 iterations. Considering an error tolerance equal to 0.01, the agents have reached the consensus with 19 and 17 iterations for the topology (a) and (b), respectively.

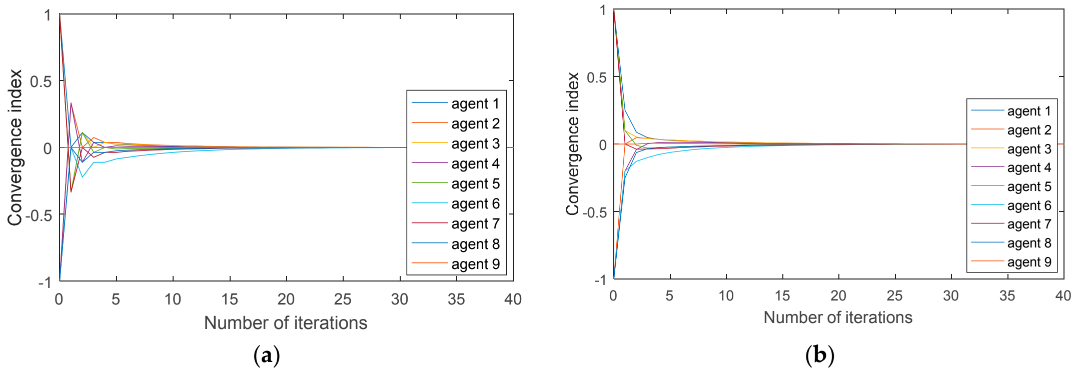


**Figure 12.** The convergence speed of the different topologies of Figure 11: (**a**) topology a; (**b**) topology b.

The time delay to reach the consensus can be estimated by:

$$T = \frac{N_{\text{iteration}} \times N_M \times N_b}{C}, \tag{14}$$

where $N_{\text{iteration}}$ is the number of required iterations to reach the consensus, $N_M$ is the size of the information matrix, $N_b$ is the number of required bits to represent each element of the information matrix, and $C$ is the communication link speed. For the topology (a) and (b), the system requires 19 and 17 iterations to converge, respectively. There are nine agents, $N_M = 9 \times 4$, and if 16 bits are used for representing each element of the information matrix, for a network with 5 Mbit/s, time delay for reaching the consensus for the topology (a), (b) are 0.002189 s and 0.001958 s, respectively. This time delay is very small compared with the pre-defined interruption time used in the decision making process. In the simulations, the interruption time is considered equal to 4 s. Therefore, the time delay for reaching the consensus can be neglected.

In order to provide the black start capability for the studied MG, the microturbine is equipped with the battery storage in the DC link, and its inverter operates in the grid-forming control mode. The inverters of the fuel cell and PVs systems operate in the grid following control mode. The wind turbine is connected directly to the grid through an induction generator. It should be noted that the secondary control is carried out locally by using a PI controller at microturbine control system aiming to restore the frequency and voltage to the nominal value after any restoration action. The restoration process is started with forming the initial information matrices of the agents. The initial information matrices are as follows:

$$\mathbf{M_1} = \begin{bmatrix} 0 & 1 & -5 & 2 \\ 0 & 0 & 0 & 0 \\ 0 & 0 & 0 & 0 \\ 0 & 0 & 0 & 0 \\ 0 & 0 & 0 & 0 \\ 0 & 0 & 0 & 0 \\ 0 & 0 & 0 & 0 \\ 0 & 0 & 0 & 0 \\ 0 & 0 & 0 & 0 \end{bmatrix}, \mathbf{M_2} = \begin{bmatrix} 0 & 0 & 0 & 0 \\ 0 & 2 & -40 & 1 \\ 0 & 0 & 0 & 0 \\ 0 & 0 & 0 & 0 \\ 0 & 0 & 0 & 0 \\ 0 & 0 & 0 & 0 \\ 0 & 0 & 0 & 0 \\ 0 & 0 & 0 & 0 \\ 0 & 0 & 0 & 0 \end{bmatrix}, \mathbf{M_3} = \begin{bmatrix} 0 & 0 & 0 & 0 \\ 0 & 0 & 0 & 0 \\ 0 & 3 & 30 & 0 \\ 0 & 0 & 0 & 0 \\ 0 & 0 & 0 & 0 \\ 0 & 0 & 0 & 0 \\ 0 & 0 & 0 & 0 \\ 0 & 0 & 0 & 0 \\ 0 & 0 & 0 & 0 \end{bmatrix}, \mathbf{M_4} = \begin{bmatrix} 0 & 0 & 0 & 0 \\ 0 & 0 & 0 & 0 \\ 0 & 0 & 0 & 0 \\ 0 & 4 & 20 & 0 \\ 0 & 0 & 0 & 0 \\ 0 & 0 & 0 & 0 \\ 0 & 0 & 0 & 0 \\ 0 & 0 & 0 & 0 \\ 0 & 0 & 0 & 0 \end{bmatrix}, \mathbf{M_5} = \begin{bmatrix} 0 & 0 & 0 & 0 \\ 0 & 0 & 0 & 0 \\ 0 & 0 & 0 & 0 \\ 0 & 0 & 0 & 0 \\ 0 & 5 & 10 & 0 \\ 0 & 0 & 0 & 0 \\ 0 & 0 & 0 & 0 \\ 0 & 0 & 0 & 0 \\ 0 & 0 & 0 & 0 \end{bmatrix}$$

$$\mathbf{M_6} = \begin{bmatrix} 0 & 0 & 0 & 0 \\ 0 & 0 & 0 & 0 \\ 0 & 0 & 0 & 0 \\ 0 & 0 & 0 & 0 \\ 0 & 0 & 0 & 0 \\ 0 & 6 & -20 & 0 \\ 0 & 0 & 0 & 0 \\ 0 & 0 & 0 & 0 \\ 0 & 0 & 0 & 0 \end{bmatrix}, \mathbf{M_7} = \begin{bmatrix} 0 & 0 & 0 & 0 \\ 0 & 0 & 0 & 0 \\ 0 & 0 & 0 & 0 \\ 0 & 0 & 0 & 0 \\ 0 & 0 & 0 & 0 \\ 0 & 0 & 0 & 0 \\ 0 & 7 & -4.8 & 0 \\ 0 & 0 & 0 & 0 \\ 0 & 0 & 0 & 0 \end{bmatrix}, \mathbf{M_8} = \begin{bmatrix} 0 & 0 & 0 & 0 \\ 0 & 0 & 0 & 0 \\ 0 & 0 & 0 & 0 \\ 0 & 0 & 0 & 0 \\ 0 & 0 & 0 & 0 \\ 0 & 0 & 0 & 0 \\ 0 & 0 & 0 & 0 \\ 0 & 8 & -20 & 0 \\ 0 & 0 & 0 & 0 \end{bmatrix}, \mathbf{M_9} = \begin{bmatrix} 0 & 0 & 0 & 0 \\ 0 & 0 & 0 & 0 \\ 0 & 0 & 0 & 0 \\ 0 & 0 & 0 & 0 \\ 0 & 0 & 0 & 0 \\ 0 & 0 & 0 & 0 \\ 0 & 0 & 0 & 0 \\ 0 & 0 & 0 & 0 \\ 0 & 9 & 15 & 0 \end{bmatrix}$$

By using ACA for the topology (a), after 0.002189 s, the agents share the initial information and reach the consensus. The final converged matrix that is available for all agents is as follows:

$$\mathbf{M_{conv.}} = \begin{bmatrix} 0 & 0 & 0 & 0 & 0 & 0 & 0 & 0 & 0 \\ \frac{1}{9} & \frac{2}{9} & \frac{3}{9} & \frac{4}{9} & \frac{5}{9} & \frac{6}{9} & \frac{7}{9} & \frac{8}{9} & \frac{9}{9} \\ \frac{-5}{9} & \frac{-40}{9} & \frac{30}{9} & \frac{20}{9} & \frac{10}{9} & \frac{-20}{9} & \frac{-4.8}{9} & \frac{-20}{9} & \frac{15}{9} \\ \frac{2}{9} & \frac{1}{9} & 0 & 0 & 0 & 0 & 0 & 0 & 0 \end{bmatrix}^{T}$$

By checking the first and the second columns of $\mathbf{M_{conv.}}$ (or second row of $\mathbf{M^T_{conv.}}$), it can be found that all of the loads and generations are disconnected, and they are ready to be restored. Column 3 shows that the MC-agents have no predefined priority and they will be chosen based on their production capacity. Among the LC-agents, the LC-agent 2 (correspond to the apartment building disconnected from bus 4) has the highest priority to be connected. LC-agent 1 (correspond to the motor load) has the next priority, and the other LC-agents have no pre-defined priority for restoration. The first common decision of the agents in this step is to connect the MC-agent 3 (correspond to the microturbine) for energizing the MG feeder.

After connecting the microturbine and passing the interruption time (4 s), the initial information matrices are again formed. All of the initial matrices are same as the previous step except the initial matrix corresponds to the MC-agent 3. In this step, the final converged matrix is as follows:

$$\mathbf{M_{conv.}} = \begin{bmatrix} 0 & 0 & 1 & 0 & 0 & 0 & 0 & 0 & 0 \\ \frac{1}{9} & \frac{2}{9} & 0 & \frac{4}{9} & \frac{5}{9} & \frac{6}{9} & \frac{7}{9} & \frac{8}{9} & \frac{9}{9} \\ \frac{-5}{9} & \frac{-40}{9} & \frac{30}{9} & \frac{20}{9} & \frac{10}{9} & \frac{-20}{9} & \frac{-4.8}{9} & \frac{-20}{9} & \frac{15}{9} \\ \frac{2}{9} & \frac{1}{9} & 0 & 0 & 0 & 0 & 0 & 0 & 0 \end{bmatrix}^{T}$$

From the above matrix, it can be seen that the microturbine has 30 kW capacity for supplying the loads. By considering the priority of the loads, the LC-agent 2 connects three apartment buildings and the microturbine will reach its capacity limit. After passing the interruption time, the initial information matrices are again formed, and the final converged matrix is expressed as follows:

$$\mathbf{M}_{\mathbf{conv.}} = \begin{bmatrix} 0 & 0 & 1 & 0 & 0 & 0 & 0 & 0 & 0 \\ \frac{1}{9} & \frac{2}{9} & 0 & \frac{4}{9} & \frac{5}{9} & \frac{6}{9} & \frac{7}{9} & \frac{8}{9} & \frac{9}{9} \\ \frac{-5}{9} & \frac{-10}{9} & 0 & \frac{20}{9} & \frac{10}{9} & \frac{-20}{9} & \frac{-4.8}{9} & \frac{-20}{9} & \frac{15}{9} \\ \frac{2}{9} & \frac{1}{9} & 0 & 0 & 0 & 0 & 0 & 0 & 0 \end{bmatrix}^{\mathrm{T}}$$

The above matrix shows that the microturbine has reached its capacity limit and there is a need for connection of another MC-agent to release the capacity of the microturbine. In this step, among the MC-agents, the MC-agent 4 (correspond to the wind turbine) that has a higher production capacity is chosen to be connected. In the next step, the final converged matrix is as follows:

$$\mathbf{M}_{\mathbf{conv.}} = \begin{bmatrix} 0 & 0 & 1 & 1 & 0 & 0 & 0 & 0 & 0 \\ \frac{1}{9} & \frac{2}{9} & 0 & 0 & \frac{5}{9} & \frac{6}{9} & \frac{7}{9} & \frac{8}{9} & \frac{9}{9} \\ \frac{-5}{9} & \frac{-10}{9} & \frac{20}{9} & 0 & \frac{10}{9} & \frac{-20}{9} & \frac{-4.8}{9} & \frac{-20}{9} & \frac{15}{9} \\ \frac{2}{9} & \frac{1}{9} & 0 & 0 & 0 & 0 & 0 & 0 & 0 \end{bmatrix}^{\mathrm{T}}$$

In this step, the microturbine has 20 kW free capacity. The remaining load of LC-agent 2 along with the LC-agent 1 and one of the residence groups correspond to the LC-agent 6 are connected. This process will continue until all of the MC-agents are connected, and the microturbine operates in its capacity limits. The remaining disconnected loads will be supplied when the MG is connected to the upstream network. Table 1 shows the sequence of restoration actions carried out based on the proposed decentralized multi-agent based scheme.

**Table 1.** Sequence of restoration actions.

| Steps | Actions | time |
|---|---|---|
| Step 1 | Connection of microturbine | $t = 1$ s |
| Step 2 | Connection of three apartment buildings at bus 4 | $t = 5$ s |
| Step 3 | Connection of wind turbine | $t = 9$ s |
| Step 4 | Connection of one apartment building at bus 4 | $t = 13$ s |
| | Connection of motor load | |
| | Connection of one of the residence groups at bus 6 | |
| Step 5 | Connection of fuel cell | $t = 17$ s |
| Step 6 | Connection of three remaining residences at bus 6 | $t = 21$ s |
| Step 7 | Connection of PVs | $t = 25$ s |
| Step 8 | Connection of one apartment building at bus 9 | $t = 29$ s |

After step 8, the final converged matrix is expressed as follows:

$$\mathbf{M}_{\mathbf{conv.}} = \begin{bmatrix} 1 & 1 & 1 & 1 & 1 & 1 & 0 & 0 & 1 \\ 0 & 0 & 0 & 0 & 0 & 0 & \frac{7}{9} & \frac{8}{9} & 0 \\ 0 & 0 & 0 & 0 & 0 & 0 & \frac{-4.8}{9} & \frac{-10}{9} & 0 \\ 0 & 0 & 0 & 0 & 0 & 0 & 0 & 0 & 0 \end{bmatrix}^{\mathrm{T}}$$

By checking the first column of $\mathbf{M}_{\mathbf{conv.}}$, it can be found that all of the generation units and loads are connected, except the load at bus 8 and a part of the load at bus 9. The microturbine also has reached its capacity limits, so the remaining loads will be supplied when the upstream network is available. At this point, the work of the proposed decentralized multi-agent based restoration scheme has been completed.

It should be noted that during the restoration procedure, if the produced (consumed) power of the generation units (loads) changes or they are not ready to be restored, the restoration decisions may be changed by providing a proper local initial information matrix. That's why it is emphasized that the proposed method uses online information of the system to determine the sequence of the restoration actions.

Dynamic simulations are carried out in the Matlab-Simulink environment. Figure 13 shows the microturbine real power during the restoration process. Each time that the loads are connected, the microturbine reaches to its capacity limit, and with the connection of generation units, its capacity is released. Figure 14 shows the frequency of the MG during the restoration process. The real power of the microsources is shown in Figure 15. The results show that for successful implementation of the proposed scheme, the generation unit with grid-forming inverter plays a key role and the proper time interval among the restoration actions is required.

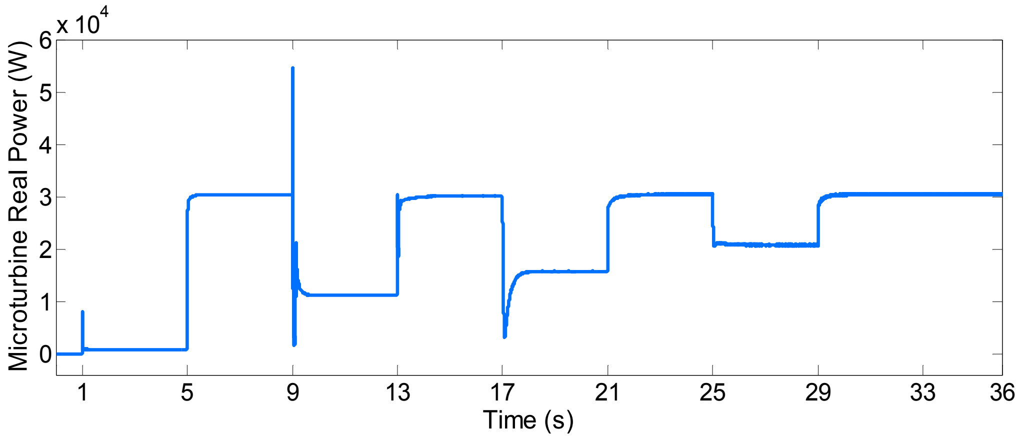


**Figure 13.** Microturbine real power during the restoration process.

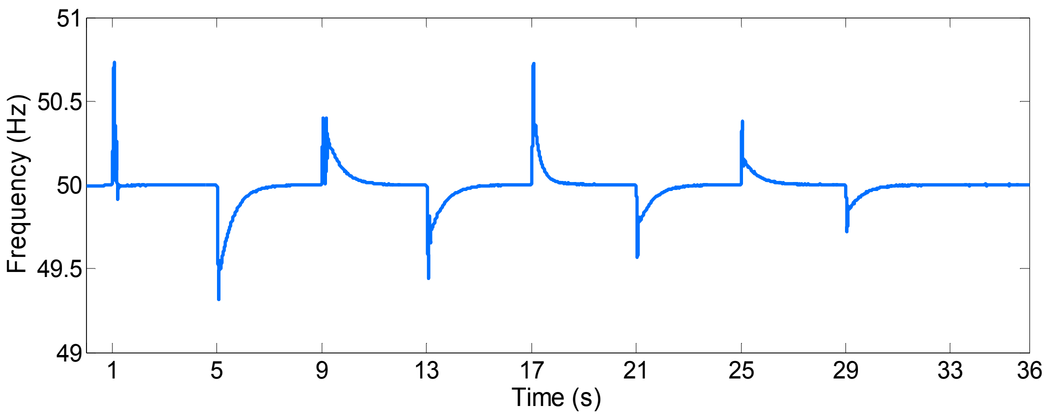


**Figure 14.** Frequency of the MG during the restoration process.

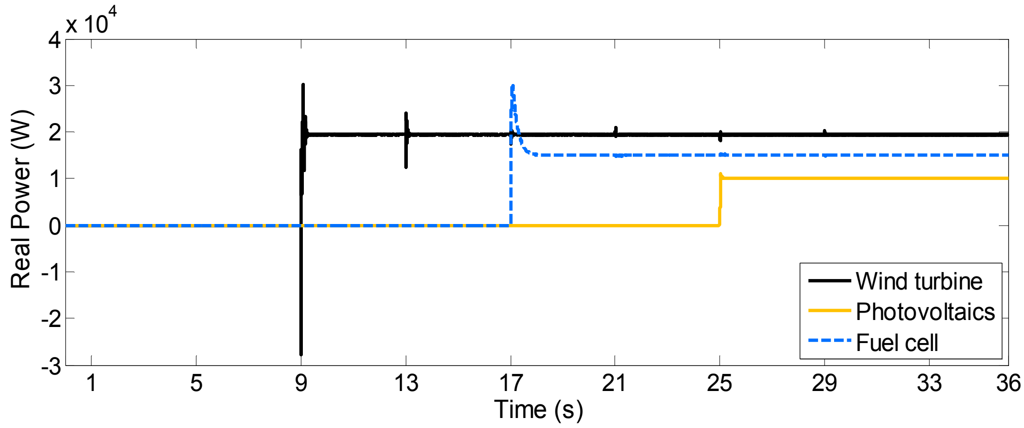


**Figure 15.** Real power of the microsources.

## 6. Conclusions

This paper proposed a decentralized multi-agent-based approach for MG restoration. In the proposed scheme, the MG local controllers were assigned to specific agents. The communication rule for sharing the local information of the agents and getting access to the global information was based on ACA. A proper restoration decisions strategy based on the discovered global information was developed. Compared to the centralized restoration schemes, the proposed method had the capability of surviving the single-point failure. Moreover, the online information of the generation/consumption of the MG was used to determine the proper sequence of restoration actions. The effectiveness of the proposed strategy is verified using a benchmark LV MG network.

**Acknowledgments:** João P. S. Catalão acknowledges the support by FEDER funds through COMPETE 2020 and by Portuguese funds through FCT, under Projects SAICT-PAC/0004/2015—POCI-01-0145-FEDER-016434, POCI-01-0145-FEDER-006961, UID/EEA/50014/2013, UID/CEC/50021/2013, and UID/EMS/00151/2013, and also funding from the EU 7th Framework Programme FP7/2007–2013 under GA No. 309048.

**Author Contributions:** All authors have worked on this manuscript together and all authors have read and approved the final manuscript.

**Conflicts of Interest:** The authors declare no conflict of interest.

## References

1. Allen, E.H.; Stuart, R.B.; Wiedman, T.E. No Light in August: Power System Restoration Following the 2003 North American Blackout. *IEEE Power Energy Mag.* **2014**, *12*, 24–33. [CrossRef]
2. Xue, Y.; Xiao, S. Generalized congestion of power systems: Insights from the massive blackouts in India. *J. Mod. Power Syst. Clean Energy* **2013**, *1*, 91–100. [CrossRef]
3. Andrews, C.J.; Arsanjani, F.; Lanier, M.W.; Miller, J.M.; Volkmann, T.A.; Wrubel, J. Special considerations in power system restoration. *IEEE Trans. Power Syst.* **1992**, *7*, 1419–1427. [CrossRef]
4. Adibi, M.M. A Framework for Power System Restoration Following a Major Power Failure. In *Power System Restoration: Methodologies amp, Implementation Strategies*; Wiley-IEEE Press: Hoboken, NJ, USA, 2000; pp. 96–101. ISBN 978-0-470-54560-7.
5. Adibi, M.M.; Fink, L.H. Power system restoration planning. *IEEE Trans. Power Syst.* **1994**, *9*, 22–28. [CrossRef]
6. Adibi, M.M.; Kafka, R.J. Power system restoration issues. *IEEE Comput. Appl. Power* **1991**, *4*, 19–24. [CrossRef]
7. Adibi, M.M.; Kafka, L.R.J.; Milanicz, D.P. Expert system requirements for power system restoration. *IEEE Trans. Power Syst.* **1994**, *9*, 1592–1600. [CrossRef]
8. Moreira, C.L.; Resende, F.O.; Lopes, J.A.P. Using Low Voltage MicroGrids for Service Restoration. *IEEE Trans. Power Syst.* **2007**, *22*, 395–403. [CrossRef]
9. Lasseter, R.H. Smart Distribution: Coupled Microgrids. *Proc. IEEE* **2011**, *99*, 1074–1082. [CrossRef]
10. Kleinberg, M.R.; Miu, K.; Chiang, H.D. Improving Service Restoration of Power Distribution Systems Through Load Curtailment of In-Service Customers. *IEEE Trans. Power Syst.* **2011**, *26*, 1110–1117. [CrossRef]

11. Liang, C.; Khodayar, M.; Shahidehpour, M. Only Connect: Microgrids for Distribution System Restoration. *IEEE Power Energy Mag.* **2014**, *12*, 70–81. [CrossRef]
12. Ancona, J.J. A framework for power system restoration following a major power failure. *IEEE Trans. Power Syst.* **1995**, *10*, 1480–1485. [CrossRef]
13. Van Hentenryck, P.; Coffrin, C. Transmission system repair and restoration. *Math. Program.* **2015**, *151*, 347–373. [CrossRef]
14. He, X.; Liao, Z.; Guo, W.; Wen, F.; Liang, J.; Fu, J. A multi-objective model for transmission network restoration based on multi-agent and tabu search. In Proceedings of the Third International Conference on Electric Utility Deregulation and Restructuring and Power Technologies, Nanjing, China, 6–9 April 2008; pp. 2392–2397.
15. Iwasaki, K.; Aoki, H. Service restoration problem in distribution power system using improved ga. *Electr. Eng. Jpn.* **2009**, *166*, 10–19. [CrossRef]
16. Pham, T.T.H.; Besanger, Y.; Hadjsaid, N. New Challenges in Power System Restoration with Large Scale of Dispersed Generation Insertion. *IEEE Trans. Power Syst.* **2009**, *24*, 398–406. [CrossRef]
17. Gu, X. Others Reconfiguration of network skeleton based on discrete particle-swarm optimization for black-start restoration. In Proceedings of the Power Engineering Society General Meeting, Montreal, QC, Canada, 18–22 June 2006.
18. Liu, Q.; Shi, L.; Zhou, M.; Li, G.; Ni, Y. A new solution to generators start-up sequence during power system restoration. In Proceedings of the Third International Conference on Electric Utility Deregulation and Restructuring and Power Technologies, Nanjing, China, 6–9 April 2008; pp. 2845–2849.
19. Adibi, S.W.M. An Approach to Standing Phase Angle Reduction A report by the Power System Restoration Working Group. *Power Syst. Restor. Methodol. Implement. Strateg.* **2000**, 142–150.
20. Mota, A.A.; Mota, L.T.M.; Morelato, A. Restoration building blocks identification using a heuristic search approach. In Proceedings of the Power Engineering Society General Meeting, Montreal, QC, Canada, 18–22 June 2006.
21. Kostic, T.; Cherkaoui, R.; Germond, A.; Pruvot, P. Decision aid function for restoration of transmission power systems: conceptual design and real time considerations. *IEEE Trans. Power Syst.* **1998**, *13*, 923–929. [CrossRef]
22. Resende, F.O.; Gil, N.J.; Lopes, J.A.P. Service restoration on distribution systems using Multi-MicroGrids. *Eur. Trans. Electr. Power.* **2011**, *21*, 1327–1342. [CrossRef]
23. Choo, Y.C.; Lai, K.X.; Kashem, M.A.; Negnevitsky, M. MicroGrid (MV Network) restoration using distributed resources after major emergencies. In Proceedings of the Australasian Universities Power Engineering Conference (AUPEC), Hobart, Tasmania, Australia, 25–28 September 2005; Volume 1, pp. 99–104.
24. Wooldridge, M. *An Introduction to Multiagent Systems*; John Wiley & Sons: New York, NY, USA, 2009.
25. Chazelle, B. An Algorithmic Approach to Collective Behavior. *J. Stat. Phys.* **2015**, *158*, 514–548. [CrossRef]
26. Hatano, Y.; Mesbahi, M. Agreement over random networks. *IEEE Trans. Autom. Control* **2005**, *50*, 1867–1872. [CrossRef]
27. Wu, J.; Meng, Z.; Yang, T.; Shi, G.; Johansson, K.H. Sampled-Data Consensus over Random Networks. *IEEE Trans. Signal Process.* **2015**, *64*, 4479–4492. [CrossRef]
28. Xue, R.; Cai, G.; Xue, R.; Cai, G. Formation Flight Control of Multi-UAV System with Communication Constraints. *J. Aerosp. Technol. Manag.* **2016**, *8*, 203–210. [CrossRef]
29. Zhang, H.; Gurfil, P. Cooperative control of multiple satellites via consensus. In Proceedings of the 24th Mediterranean Conference on Control and Automation (MED), Athens, Greece, 21–24 June 2016; pp. 1102–1107.
30. Montijano, E.; Thunberg, J.; Hu, X.; Sagüés, C. Epipolar Visual Servoing for Multirobot Distributed Consensus. *IEEE Trans. Robot.* **2013**, *29*, 1212–1225. [CrossRef]
31. Grandi, R.; Falconi, R.; Melchiorri, C. Coordination and control of autonomous mobile robot groups using a hybrid technique based on Particle Swarm Optimization and Consensus. In Proceedings of the International Conference on Robotics and Biomimetics (ROBIO), Shenzhen, China, 12–14 December 2013; pp. 1514–1519.
32. Rokrok, E.; Golshan, M.E.H. Adaptive voltage droop scheme for voltage source converters in an islanded multibus microgrid. *IET Gener. Transm. Distrib.* **2010**, *4*, 562–578. [CrossRef]
33. Katiraei, F.; Iravani, R.; Hatziargyriou, N.; Dimeas, A. Microgrids management. *IEEE Power Energy Mag.* **2008**, *6*, 54–65. [CrossRef]

34. Bidram, A.; Davoudi, A. Hierarchical Structure of Microgrids Control System. *IEEE Trans. Smart Grid.* **2012**, *3*, 1963–1976. [CrossRef]
35. Lopes, J.P.; Moreira, C.L.; Madureira, A.G. Defining control strategies for microgrids islanded operation. *IEEE Trans. Power Syst.* **2006**, *21*, 916–924. [CrossRef]
36. Nagpal, M.; Moshref, A.; Morison, G.K.; Kundur, P. Experience with testing and modeling of gas turbines. In Proceedings of the Power Engineering Society Winter Meeting, Columbus, OH, USA, 28 January–1 February 2001; pp. 652–656.
37. Kim, I.-S. Robust maximum power point tracker using sliding mode controller for the three-phase grid-connected photovoltaic system. *Sol. Energy.* **2007**, *81*, 405–414. [CrossRef]
38. González-Longatt, F.; Amaya, O.; Cooz, M.; Duran, L. Dynamic behavior of constant speed wt based on induction generator directly connected to grid. In Proceedings of the 6th World Wind Energy Conference and Exhibition (WWEC), Buenos Aires, Argentina, 2–4 October 2007.
39. Zhu, Y.; Tomsovic, K. Development of models for analyzing the load-following performance of microturbines and fuel cells. *Electr. Power Syst. Res.* **2002**, *62*, 1–11. [CrossRef]
40. Padulles, J.; Ault, G.W.; McDonald, J.R. An integrated SOFC plant dynamic model for power systems simulation. *J. Power Sources* **2000**, *86*, 495–500. [CrossRef]
41. Palizban, O.; Kauhaniemi, K. Hierarchical control structure in microgrids with distributed generation: Island and grid-connected mode. *Renew. Sustain. Energy Rev.* **2015**, *44*, 797–813. [CrossRef]
42. Wang, Y.; Dong, X.; Wang, B.; Liu, J.; Guo, A.X. Black start studies for micro-grids with distributed generators. In Proceedings of the 12th IET International Conference on Developments in Power System Protection (DPSP 2014), Copenhagen, Denmark, 31 March–3 April 2014.
43. Rocabert, J.; Luna, A.; Blaabjerg, F.; Rodríguez, P. Control of Power Converters in AC Microgrids. *IEEE Trans. Power Electron.* **2012**, *27*, 4734–4749. [CrossRef]
44. Xiao, L.; Boyd, S. Fast linear iterations for distributed averaging. *Syst. Control Lett.* **2004**, *53*, 65–78. [CrossRef]
45. Marshall, A.W.; Olkin, I.; Arnold, B.C. Doubly Stochastic Matrices. Inequalities: Theory of Majorization and Its Applications. In *Springer Series in Statistics*; Springer: New York, NY, USA, 2010; pp. 29–77. ISBN 978-0-387-40087-7.
46. Horn, R.A.; Johnson, C.R. *Matrix Analysis*, 2nd ed.; Cambridge University Press: Cambridge, UK, 2012.
47. Xiao, L.; Boyd, S.; Kim, S.-J. Distributed average consensus with least-mean-square deviation. *J. Parallel Distrib. Comput.* **2007**, *67*, 33–46. [CrossRef]
48. Papathanassiou, S.; Hatziargyriou, N.; Strunz, K. Others A benchmark low voltage microgrid network. In Proceedings of the CIGRE Symposium: Power Systems with Dispersed Generation, Athens, Greece, 16–20 April 2005; pp. 1–8.